Carapace bone histology in the giant pleurodiran turtle *Stupendemys geographicus*: Phylogeny and function

TORSTEN M. SCHEYER and MARCELO R. SÁNCHEZ-VILLAGRA

Scheyer, T.M. and Sánchez-Villagra, M.R. 2007. Carapace bone histology in the giant pleurodiran turtle *Stupendemys geographicus*: Phylogeny and function. *Acta Palaeontologica Polonica* 52 (1): 137–154.

Stupendemys geographicus (Pleurodira: Pelomedusoides: Podocnemidae) is a giant turtle from the Miocene of Venezuela and Brazil. The bone histology of the carapace of two adult specimens from the Urumaco Formation is described herein, one of which is the largest of this species ever found. In order to determine phylogenetic versus scaling factors influencing bone histology, *S. geographicus* is compared with related podocnemid *Podocnemis erythrocephala*, and with fossil and Recent pelomedusoides taxa *Bothremys barberi*, *Taphrosphys sulcatus*, "*Foxemys* cf. *F. mechinorum*", and *Pelomedusa subrufa*. Potential scaling effects on bone histology were further investigated by comparison to the Pleistocene giant tortoise *Hesperotestudo* (*Caudochelys*) *crassiscutata* and the Late Cretaceous marine protostegid turtle *Archelon ischyros*. A diploe structure of the shell with well developed external and internal cortices framing interior cancellous bone is plesiomorphic for all sampled taxa. Similarly, the occurrence of growth marks in the shell elements is interpreted as plesiomorphic, with the sampled neural elements providing the most extensive record of growth marks. The assignment of *S. geographicus* to the Podocnemidae was neither strengthened nor refuted by the bone histology. A reduced thickness of the internal cortex of the shell elements constitutes a potential synapomorphy of the Bothremydidae. *S. geographicus* and *H. crassiscutata* both express extensive weight-reduction through lightweight-construction while retaining form stability of the shell. The bone histology of *A. ischyros* presents features likely related to an open marine lifestyle.

Key words: Testudines, Pleurodira, Pelomedusoides, Bothremydidae, Podocnemidae, *Stupendemys geographicus*, bone histology, Miocene, Venezuela.

Torsten M. Scheyer [tscheyer@uni-bonn.de], Institute of Paleontology, University of Bonn, Nussallee 8, D-53115 Bonn, Germany, current address: Paläontologisches Institut und Museum, Universität Zürich, Karl Schmid-Strasse 4, CH-8006 Zürich, Switzerland;
Marcelo R. Sánchez-Villagra [m.sanchez@pim.unizh.ch], Paläontologisches Institut und Museum, Universität Zürich, Karl Schmid-Strasse 4, CH-8006 Zürich, Switzerland.

Introduction

Although the bone histology is a field with longstanding tradition in biology and paleontology, the analysis of bone microstructures of dermal bone and of osteoderms has just come recently into focus. In their studies on thyreophoran dinosaurs and other armor-bearing amniotes, Ricqlès et al. (2001), Barrett et al. (2002), Scheyer and Sander (2004), and Main et al. (2005) gave detailed comparative accounts of osteoderm histology, concluding that metaplastic ossification (Haines and Mohuiddin 1968) led to the formation of these dermal bones. Thus the development and bone microstructures of dermal bone and osteoderms differ strongly from those of endoskeletal bones, e.g., long bones. From the paleontological perspective, the insight that dermal bone and osteoderms are of metaplastic origin means that aspects of dermal soft tissue can be reconstructed as shown in recent studies of soft-shelled turtles (Scheyer et al. in press) and ankylosaurian dinosaurs (Scheyer and Sander 2004). At the same time, integumentary structures and, especially, morphological and histological characteristics of tetrapod osteoderms were recognized as valuable assets for developing phylogenetic hypotheses for the major amniote groups (Scheyer and Sander 2004; Hill 2005; Scheyer et al. in press).

The unique body bauplan of turtles, i.e., the encasement of the body within a rigid shell, thus has prompted us to further investigate the bone histological nature of the turtle shell as a composite structure of endoskeletal and dermal bone (e.g., Vallén 1942; Zangerl 1969; Ewert 1985) in a comprehensive survey of turtle shell bone histology including about 100 fossil and Recent turtle and 18 outgroup taxa. The current study is part of this survey.

Stupendemys geographicus Wood, 1976 (Pleurodira: Podocnemidae) is a giant turtle from late Miocene deposits of Venezuela and Brazil (Wood 1976; Lapparent de Broin et al. 1993; Gaffney et al. 1998). Wood (1976) described this species based on fairly complete shell material from the late Miocene Urumaco Formation in Venezuela, as the "world's largest turtle". Previously thought to represent a marine form by Wood (1976), *S. geographicus* was regarded by Lapparent de Broin et al. (1993) as primarily inhabiting freshwater. In fact, the largest excavated specimen of this species co-

mes from Urumaco and has a straight carapace length (SCL) of 3.3 meters and a maximum carapace width (MCW) of 2.18 meters (Aguilera et al. 1994; Aguilera 2004). Only few other turtles, such as the marine protostegid turtle *Archelon ischyros* Wieland, 1896 from the Late Cretaceous of North America and the trionychid *Drazinderetes tethyensis* Head et al., 1999 from the Eocene of Pakistan also reached giant dimensions (Wieland 1896; Head et al. 1999; Shimada and Hooks 2004).

Body size is a fundamental variable correlated with a large variety of aspects of the life history and anatomy of organisms, including bone structure (e.g., Klingenberg 1998; Liem et al. 2001). The structure of the turtle shell bone is also likely to be determined by size, and constrained by phylogenetic history. Bone histology can be influenced by size- and age-related factors, as discussed by Hailey and Lambert (2002) in a study of phenotypic and genetic differences in the growth of giant Afrotropical tortoises. In this context, the study of species at the end of the spectrum of size variation is of special interest. This paper focuses on how the bone histology of *Stupendemys geographicus* is influenced by phylogenetic and functional size/age-related constraints.

To test hypotheses with the bone histological data obtained from our study, the thin-sections of *S. geographicus* were compared with representatives of Pelomedusoides, as well as with other giant turtle taxa, namely the land-dwelling tortoise *Hesperotestudo* (*Caudochelys*) *crassiscutata* (Leidy, 1889) from the Pleistocene of Florida, USA (see Meylan 1995), and the aforementioned marine turtle *Archelon ischyros* Wieland, 1896.

Relevant for the comparison with *S. geographicus* are other representatives of Pelomedusoides (Broin 1988). In what follows, we clarify the use of some taxonomic terms and provide some basic background important to the understanding of the phylogenetic and functional comparisons undertaken in this study (Fig. 1).

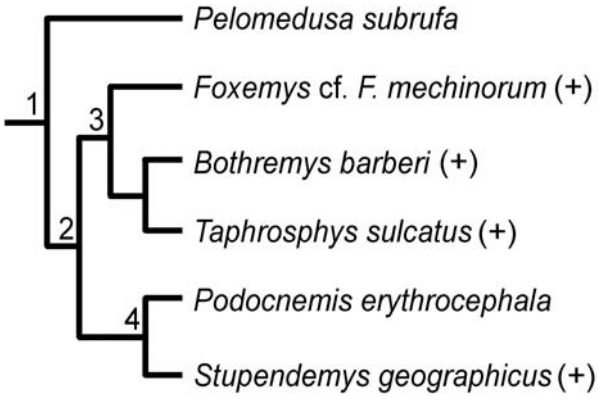

Fig. 1. Phylogenetic working-hypothesis of the sampled pelomedusoid turtle taxa (Pleurodira: Pelomedusoides) based on Antunes and Broin (1988), Broin (1988), Meylan (1996), and Tong et al. (1998). Fossil taxa are indicated by a small cross in parentheses and numbers are applied for higher taxa names. 1, Pelomedusoides; 2, Podocnemoidae; 3, Bothremydidae; 4, Podocnemidae.

Podocnemidae.—Podocnemidae comprises South American and African taxa and probably originated in the Late Cretaceous (Gaffney and Forster 2003; see Joyce at al. 2004 for discussion). *S. geographicus*, for which the complete skull is yet unknown (e.g., Gaffney et al. 1998), is included in Podocnemidae (Fig. 1) based on morphological characters of the postcranium, especially on the saddle-shaped central articulations of the cervicals (Wood 1976; Lapparent de Broin et al. 1993). As another representative of Podocnemidae, *Podocnemis erythrocephala* (Spix, 1824), a small living relative of *S. geographicus* from the northern parts of South America (Ernst and Barbour 1989) that can reach a SCL of about 300 mm, was sampled. *Podocnemis* spp. and *S. geographicus,* among other taxa, may belong to a less inclusive taxon, Podocnemidinae, within Podocnemidae (e.g., Lapparent de Broin et al. 1993; Fuente 2003).

Podocnemoidae.—According to Meylan (1996) and Noonan (2000), Podocnemidae together with the fossil clade Bothremydidae form Podocnemoidae. Specimens of *Taphrosphys sulcatus* (Leidy, 1856), *Bothremys barberi* (Schmidt, 1940), and of "*Foxemys* cf. *F. mechinorum*" Tong, Gaffney, and Buffetaut, 1998 = *Polysternon mechinorum* (Tong, Gaffney, and Buffetaut, 1998) *fide* Lapparent de Broin (2001) were sectioned to sample Bothremydidae (see also Gaffney and Zangerl 1968; Gaffney 1975; Tong and Gaffney 2000). The first two species are well known from Late Cretaceous marine sediments of North America (e.g., New Jersey). The last taxon, "*Foxemys*", derives from Late Cretaceous (early Maastrichtian) fluvial sediments near Cruzy, Hérault, southern France. According to Tong et al. (1998), "*Foxemys* cf. *F. mechinorum*" is tentatively assigned as a basal bothremydid and is thus treated as sister taxon to more derived genera *Taphrosphys*, *Bothremys*, and *Rosasia* with relationships being ("*Foxemys*" (*Taphrosphys* (*Bothremys* + *Rosasia*))). Adult bothremydid taxa can reach shell lengths of up to 1500 mm (e.g., Gaffney 2001). However, shell lengths could not be ascertained for the sampled specimens.

Pelomedusoides.—Podocnemidae, Bothremydidae, and Pelomedusidae form the clade Pelomedusoides (Antunes and Broin 1988), one of the two major crown clades of Pleurodira, the other being Chelidae. A Recent *Pelomedusa subrufa* (Bonnaterre, 1789), a small specimen with a SCL of 150 mm, was sampled as a representative for the Pelomedusidae.

Institutional abbreviations.—UNEFM-CIAPP, Centre of Archaeology, Anthropology and Paleontology of Francisco de Miranda University, Coro, Venezuela; FM, The Field Museum, Chicago, Illinois, USA; IPB, Goldfuss-Museum, Institute for Paleontology, University of Bonn, Bonn, Germany; MVZ, Museum of Zoology, University of California, Berkeley, California, USA; ROM, Royal Ontario Museum, Toronto, Ontario, Canada; YPM, Yale Peabody Museum, New Haven, Connecticut, USA.

Other abbreviations.—MCW, maximum carapace width; SCL, straight carapace length.

Table 1. Summary of the sectioned material of this study. Abbreviations: co, costal; frag., fragmentary; indet., indeterminate; n., neural; p., peripheral; pl., plastron.

Taxon	Number and kind of samples	Sampled elements	Measurements	Max. count of growth marks	Presumed age stages
Stupendemys geographicus (Podocnemidae)	UNEFM-101 (fossil) UNEFM-CIAPP-2002-01 (fossil)	1 frag. n. 2 frag. co. (A and B)	SCL: ?2000–3000 mm; lateral: 9 mm thick SCL: 3300 mm; MCW: 218 mm; A: 30 mm thick; B: 10 mm thick	8 2–4	Adult Senile adult
Podocnemis erythrocephala (Podocnemidae)	YPM 11853 (Recent; macerated)	1 n., 1 co., 1 p., 1 hypoplastron	SCL: ~180 mm; MCW: ~150 mm; max. sample thickness: 4 mm (neural)	10	Subadult
Bothremys barberi (Bothremydidae)	FM P27406 (fossil)	1 n., 1 co., 1 p., 1 pl. frag.	Lateral parts of costal and neural: ~15 mm thick	7–9	?Adult
Taphrosphys sulcatus (Bothremydidae)	YPM 40288 (fossil)	1 n., 1 co., 1 p., 1 ?hyo- or hypoplastron	Lateral parts of costal and neural: ~10 mm thick	20	?Adult
"*Foxemys* cf. *F. mechinorum*" (Bothremydidae)	IPB R559a (fossil)	1 n., 1 co., 2 pl. frag.	Elements between 4 and 7 mm thick	6	not discernable
Pelomedusa subrufa (Pelomedusidae)	MVZ 230517 (Recent; core-drilled)	1 co., 1 p., 1 hyoplastron	SCL: 155 mm; MCW: 110 mm Core diameter: ~12 mm; max. thickness of samples: 2 mm	1–2	?Subadult
Hesperotestudo crassiscutata (Testudinidae)	ROM 51460 ROM 55400 (fossil)	1 n. 1 frag. co., 1 ?p., 1 frag. xiphiplastron	Length: ~70 mm; width: 120 mm; 35 mm thick Xiphiplastron: max. 33 mm thick	?4–7	?Adult
Archelon ischyros (Protostegidae)	YPM 1783 (fossil)	1 frag. co., 1 frag. p., 1 indet. shell fragment	Costal: max. 40 mm thick Teardrop-shaped peripheral: 50 mm thick; max. 100 mm	3–4	?Subadult

Materials and methods

Two fragmentary costals (A and B) of specimen UNEFM-CIAPP-2002-01 of *Stupendemys geographicus* Wood, 1976, measuring 3300 mm in SCL and 2180 mm in MCW, were sampled (Aguilera et al. 1994). The costal fragment A from the mid-region of the carapace has an overall thickness of 30 mm, whereas fragment B from the posterior part of the carapace is significantly thinner (about 10 mm). It is assumed that both costal fragments were of similar thickness in the living turtle, thus the cortical bone and broken bone trabeculae of fragment B correspond to only the lower third part of fragment A. Additional articulated pieces of a neural from a smaller fragmentary specimen (UNEFM-101) were also obtained for sectioning. The bone histology of *Stupendemys geographicus* was thus observed in two different size categories (Fig. 2A, B). With a calculated SCL of two to three meters, the smaller specimen is situated well within the size variation of other known, certainly adult, complete specimens of *S. geographicus* (Wood 1976; Sánchez-Villagra personal observations), even though the lateral parts of the neural fragment are only a third of the thickness of costal fragment A of UNEFM-CIAPP-2002-01. Compared to the slight stages of erosion found in the neural, both costal fragments exhibit medium to strong surface damages. It thus has to be assumed that neither fragment presents the complete histological evidence of undamaged cortices. Likewise measurements of the thicknesses of all fragments give only approximate values that have to be treated with caution.

Further sampling included *Podocnemis erythrocephala* (Spix, 1824) (YPM 11853), *Bothremys barberi* (Schmidt, 1940) (FM P27406), *Taphrosphys sulcatus* (Leidy, 1856) (YPM 40288), and "*Foxemys* cf. *F. mechinorum*" Tong, Gaffney, and Buffetaut, 1998 = *Polysternon mechinorum* (Tong, Gaffney, and Buffetaut, 1998) *fide* Lapparent de Broin (2001) (IPB R559a), *Pelomedusa subrufa* (Bonnaterre, 1789) (MVZ 230517), *Hesperotestudo* (*Caudochelys*) *crassiscutata* (Leidy, 1889) (ROM 51460; ROM 55400), and *Archelon ischyros* Wieland, 1896 (YPM 1783). Table 1 presents a summary of the taxa sampled, specimen numbers, size and length measurements, estimated age stages, and growth cycle counts where applicable.

In the case of *Pelomedusa subrufa*, no complete shell elements, but drilled cores of the shell were sub-sampled. A diamond-studded core bit (14 mm in diameter) mounted on a slow-moving power-drill supported by a drill press was used to extract the keratinous shield and the underlying bone from the alcohol preserved turtle specimen (see also Sander 2000). These samples are thus the only ones herein that preserve the interface between the shield cover above, the connective tissue in between, and the bone below. A beginning fusion of its

individual bony elements is present in the carapacial disk of *Podocnemis erythrocephala*. The fusion started with the neural elements in the middle of the carapacial disc and continued towards half of the length of the costals. The distal ends of the costals and the peripherals were sutured but still unfused. The bone histology of *H. crassiscutata* was best preserved in the xiphiplastron, the peripheral, and the costal fragment, whereas the neural is diagenetically altered.

All thin-sections were prepared by TMS at the Institute of Paleontology, University of Bonn, Germany. The sampling followed standard petrographic thin-sectioning procedures as described for example in Scheyer and Sander (2004). The description of the turtle shell elements follows Zangerl (1969), and the histological descriptions are mainly based on Francillon-Vieillot et al. (1990) and Scheyer and Sander (2004). In living bone, the orientation of the collagenous fibers and fiber bundles also determines the orientation of the hydroxyl-apatite crystallites (the associated mineral phase of the bone). In the fossil bone, this crystallite orientation is retained, thus allowing the reconstruction of this soft-tissue part of the bone that is usually lost during fossilization (e.g., Francillon-Vieillot et al. (1990).

The terms "external" and "internal" are used throughout the text instead of "dorsal" and "ventral" to prevent confusion among dorsal carapacial and ventral plastral bones of the turtle shell (e.g., the "dorsal" surface of a carapace bone would be the true dorsal bone surface, while the "dorsal" surface of a plastral bone would indicate the visceral side of the shell element). The term "interior" pertains to the core or center of the shell bone (i.e., cancellous bone) that is usually framed by the external and internal cortex.

Results

Variation in bone histology observed among different shell bone elements within a taxon was uniformly connected to the differences of gross morphology of the respective elements. Otherwise, the bone histology was conspicuously consistent for each taxon. However, differences due to sexual dimorphism, especially for the two size variations of *Stupendemys geographicus* could not be generally ruled out. Intraspecific variation in bone histology was not encountered partly due to the small sample size. On the other hand, it is not expected either, as major differences in the bone histology of the turtle shell seem to be expressed only on generic or even higher taxonomic levels (T. Scheyer, unpublished data).

Gross morphology of *Stupendemys geographicus* Wood, 1976.—Sutures, scute sulci, or incorporated rib parts in the case of the costal fragments, were not found in the samples. Wood (1976) postulated that it is not uncommon for *S. geographicus*, as for other larger turtles, that sutures fuse between the individual carapace bones, and are thus not recognizable from the shell surfaces. No sculpturing is apparent on the external surfaces of the fragments either. However, due to the weathering of the fragments, it could not be deduced whether the surfaces once possessed the shallow sculpturing pattern typical for "pelomedusoids" (Broin 1977; see also Meylan 1996). Assessing the exact orientation of the fragments within the carapacial disc was possible though, based on field sketches depicting the excavating. Cross-sections and longitudinal sections relative to the long axis of the carapace were made of the costal fragments. The primary plane of sectioning of the neural fragment was arranged perpendicular to the vertebral column.

Bone histology of *Stupendemys geographicus* Wood, 1976.—Both costal fragments and the neural fragment have a diploe structure (e.g., Francillon-Vieillot et al. 1990; Bloom 1994), typical for turtle shell bones, in which well developed internal and external compact bone layers frame an area of cancellous bone (see Fig. 2A, B). In all three specimens, some of the compact bone lamellae together with scattered secondary osteons observed in the external and internal cortices are partly eroded.

External cortex.—The external cortex of the costals and the neural is a compact bone layer with moderate vascularization. Right at the bone surfaces, the cortex is mainly composed of fibrous bone tissue interspersed with few primary osteons, and large scattered secondary osteons (Fig. 3A_1, A_2). Secondary osteon cluster are not developed in the external cortex. The loosely packed interwoven collagen fiber bundles in the cortical bone extend predominantly diagonally through the bone matrix towards the surface of the bone (Fig. 3A_2, A_3). Fiber bundles that extend perpendicular to the external surface of the bone are also present in the interwo-

Fig. 2. Selected photographs of the thin-sections used in this study in normal light. Cortical thicknesses are marked with a bracket. **A**. Neural of *Stupendemys geographicus* Wood, 1976 (UNEFM-101), late Miocene Urumaco Fm., Venezuela, South America. Internal and external cortices are of similar thickness. **B**. Costal fragment A of *Stupendemys geographicus* Wood, 1976 (UNEFM-CIAPP-2002-01; same provenance as in A). The plane of sectioning is perpendicular to the long-axis of the carapace (L-section). Both cortices are not clearly defined (signalized with question marks) due to diagenetic processes. **C**. Neural and costal (YPM 11853) of *Podocnemis erythrocephala* (Spix, 1824), Recent red-headed Amazon River turtle, South America (provenance unknown). Both cortices are of similar thickness. **D**. Costal (FM P27406) of *Bothremys barberi* (Schmidt, 1940), Campanian (Late Cretaceous) Mooreville Chalk, Selma Group, Dallas County, Alabama, USA. The internal cortex is reduced. **E**. Neural (YPM 40288) of *Taphrosphys sulcatus* (Leidy, 1856), Late Cretaceous, New Jersey, USA. The internal cortex is reduced. **F**. Plastral fragment (?hyo- or hypoplastron, IPB R559a) of "*Foxemys* cf. *F. mechinorum*", Late Cretaceous (early Maastrichtian), Cruzy, Hérault, southern France. The internal cortex is reduced. **G**. Drilled core of costal (MVZ 230517) of *Pelomedusa subrufa* (Bonnaterre, 1789), a Recent African helmeted turtle (provenance unknown). The keratinous shield still covers the bone. **H**. Xiphiplastron of *Hesperotestudo* (*Caudochelys*) *crassiscutata* (Leidy, 1889) (ROM 55400), Pleistocene, Florida, USA. Internal and external cortices that frame cancellous bone are of equal thickness. **I**. Shell element (YPM 1783) of *Archelon ischyros* Wieland, 1896, Late Cretaceous, South Dakota, USA. The bone tissue is uniformly cancellous. Abbreviations: CB, cancellous bone; ECO, external cortex; ICO, internal cortex; KS, keratinous shield. Scale bars 10 mm. →

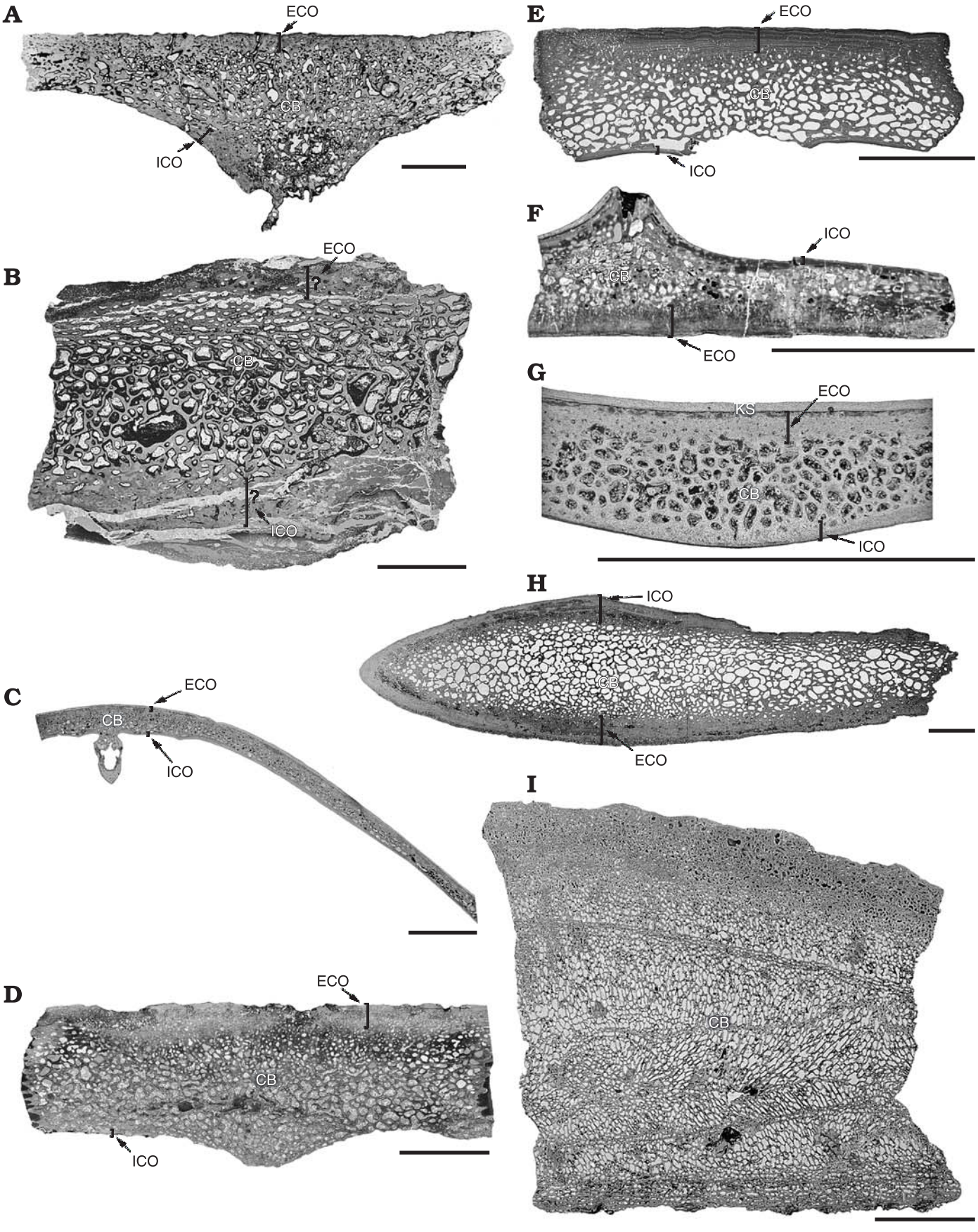
A
ECO
CB
ICO
B
ECO
?
CB
?
ICO
C
ECO
CB
ICO
D
ECO
CB
ICO
E
ECO
CB
ICO
F
ICO
CB
ECO
G
ECO
KS
CB
ICO
H
ICO
CB
ECO
I
CB

ven matrix of structural fiber bundles. Cyclical incremental growth marks within the fibrous bone tissue, distinct from lines of arrested growth of periosteal lamellar-zonal bone endoskeletal bones (Castanet et al. 1993), can be recognized in most areas of the cortex of the neural (Fig. $3A_1$), while the few growth marks in the costal fragments are mostly discontinuous and not as easily discerned. Towards the midline of the neural, growth marks are also difficult to follow, because the mid-region of the cortex of the neural is slightly crushed. A gradual increase in the amount and in size of the secondary osteons is recognized towards the internal cancellous parts of the bony plates. In the costals, vascular spaces have flattened shapes with long-axes subparallel to the external surface of the bone. In the neural though, Haversian canals of the secondary osteons are mostly round in shape with secondary osteons trending anteroposteriorly through the neural (Fig. $3A_1$, A_2). Bone cell lacunae within the cortex are mostly of a flattened and elongated shape, a fact that is usually attributed to slower bone deposition rates, i.e., in lamellar bone (e.g., Francillon-Vieillot et al. 1990). In general, the cortical bone cell lacunae bear longer canaliculi than the bone cell lacunae found in the interior cancellous bone tissue.

In the neural, Sharpey's fibers cross the interwoven structural fiber bundles of the bone tissue at moderate angles. They point towards medial on both sides of the midline. The fiber orientation could not be reconstructed in the regions right at the midline of the neural where the bone lamellae are slightly crushed. It cannot be stated with certainty whether Sharpey's fibers are also present within the external cortices of the costal fragments.

Internal cortex.—Similar to the external cortex, the internal cortex of all fragments is composed of two zones of different bone tissue. Towards the interior of the shell, the compact layer of bone is composed of scattered secondary osteons (Fig. $3B_1$) or secondary osteon clusters (Fig. $3B_2$, B_3). Towards the internal surface of the bone elements, the cortical bone constitutes fibrous bone tissue (Fig. $3B_1$). The transition between the two zones is rather sharply defined. Small pockets of primary fibrous bone tissue are also seen in spaces in between the secondary osteons (Fig. $3B_3$). The fibrous bone tissue of the internal cortex is characterized by loosely packed structural collagenous fiber bundles that are oriented either subparallel or at diagonal angles to the internal surface of the bone fragment (Fig. $3B_1$). Few collagenous structural fiber bundles, which insert perpendicular to the internal surface of the bone, cross the fibrous tissue thus creating an interwoven appearance. Due to erosion of the cortices of the costal fragments, the thickness of this internal tissue type varies strongly. Besides few scattered primary osteons and erosion cavities, the fibrous bone is mainly avascular. It could not be discerned if Sharpey's fibers sensu stricto are present within the interwoven fibrous tissue of the internal cortex of the costals.

In the neural fragment, the internal cortex is composed of scattered secondary osteons that become dense towards the midline of the fragment. The cortex appears quite massive in the areas in which they are vascularized by Haversian canals. Medially in the neural fragment, remnants of the incorporated neural arch can be observed (see Fig. 2A). The bone of the incorporated neural arch is composed of tightly clustered secondary osteons. Here, the cell lacunae have a flattened and elongated shape. The roof of the neural canal is not seen in the thin-section because the bone is damaged and eroded in this area (Fig. 2A). Sharpey's fibers crossing the structural collagenous fibers seem to be present in the areas around the incorporated neural arch, but their presence is not as conspicuous as in the external cortex. Remnants of compact bone lamellae slightly internal to the internal cortex are still traceable through the whole width of the neural fragment. These horizontally trending bone lamellae remain visible even though they have been extensively interrupted by newly formed bone trabeculae and large scattered secondary osteons.

Cancellous bone.—The cancellous bone of the costals is composed of thick trabeculae of rather uniform appearance (see Fig. 2B). Overall, the bone trabeculae and vascular spaces are evenly distributed in the cancellous bone. Only in a few cases do the spaces between the trabeculae coalesce to form larger vascular cavities. The trabeculae themselves are composed of centripetally deposited secondary bone lamellae. Towards the external and internal cortices, the vascular spaces are dorsoventrally flattened. They are rounder towards the interior of the bone. Flattened and elongated bone cell lacunae and interwoven structural fiber bundles are restricted to interstitial areas of the trabeculae where remnants of primary fibrous bone tissue are preserved (see also Fig. $3B_3$).

The cancellous interior of the neural fragment is similarly composed of short and rather thick bone trabeculae. This gives the neural a massive and moderately vascularized appearance in cross-section (see also Fig. 2A). The trabeculae become thinner and more fragile towards the internal surface of the bone. In the lower part of the neural, along the midline, the trabecular system has collapsed. The largest vascular spaces within the whole of the neural fragment are found in the center of the cancellous bone (Fig. 2A).

Bone histology of *Podocnemis erythrocephala* (Spix, 1824).—All sampled shell elements of *P. erythrocephala* have a clear diploe build where internal and external compact bone layers of similar thickness enclose a cancellous interior (Figs. 2C, 4A). The external cortices of the elements are composed of interwoven structural fiber bundles with nu-

Fig. 3. Bone histology of *Stupendemys geographicus* Wood, 1976. **A**, Sampled neural fragment (UNEFM-101) of *Stupendemys geographicus* Wood, 1976, late Miocene Urumaco Fm., Venezuela, South America. A_1. Close-up of external cortex in normal transmitted light. The cortical bone is vascularized by primary and secondary osteons. Growth marks (small white arrows) occur throughout the external cortex. A_2. Same external cortex as in A_1, seen in polarized light. The external cortex constitutes a bone matrix of interwoven structural fiber bundles with scattered primary and secondary osteons. A_3. Close-up →

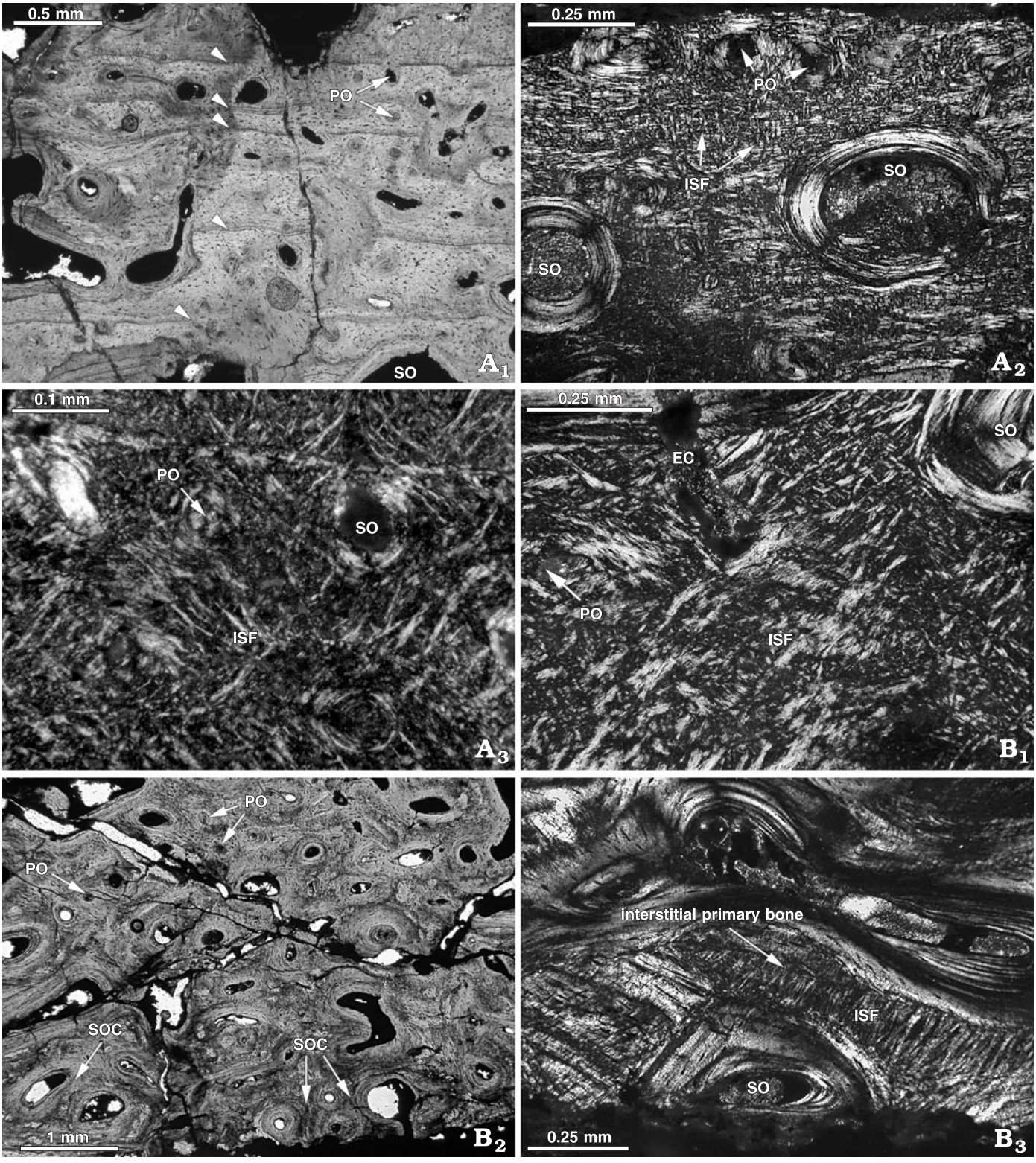

of the bone matrix of interwoven structural fiber bundles. Note that fiber bundles extend predominantly in diagonal angles towards the external surface of the bone. **B**. Sampled costal fragment A (UNEFM-CIAPP-2002-01) of *Stupendemys geographicus* Wood, 1976, late Miocene Urumaco Fm., Venezuela, South America. B_1. Internal cortex viewed in polarized light. Similar to the external cortex, the internal cortex constitutes interwoven structural fiber bundles. Fiber bundles extend mostly diagonally through the bone tissue. The cortical bone is vascularized by primary and secondary osteons and erosion cavities. B_2. Areas of strong remodeling in the internal cortex in normal transmitted light. In addition to primary osteons, the cortical bone is dominated by secondary osteon clusters. B_3. Detail of the internal cortex in polarized light. Note that interstitial areas of primary bone tissue in between the osteon clusters are also composed of interwoven structural fiber bundles. Abbreviations: EC, erosion cavity; ISF, interwoven structural collagenous fiber bundles; PO, primary osteon; SO, secondary osteon; SOC, secondary osteon cluster.

merous growth marks (Fig. 4B–D). Primary and scattered secondary osteons range throughout the whole of the external cortex, but the overall amount of both osteon types decreases towards the external surface of the bone. The arrangement of the fiber bundles within the external-most part of the external cortex is not well structured. The fiber bundles trend in an irregular fashion, with the majority being oriented diagonally towards the surface of the bone (Fig. 4D). Throughout the whole of the external cortex, extensive fiber bundles that extend perpendicular to the bone surface can be observed. The external part of the cortex is avascular. Bone cell lacunae are elongated and flattened and most have long canaliculi. The external cortex of the sampled costal further exhibits an inverted semicircular patch of secondary remodeled bone (Fig. 4B–D). Here, no growth marks within the external cortical bone are observed and the surface of the bone is indented and rugose.

The cancellous bone is dominated by short secondary trabeculae, lined with centripetally deposited lamellar bone. Elongated and flattened bone cell lacunae that lack canaliculi are abundant within the trabecular bone lamellae. The cancellous bone is replaced by scattered secondary osteons (Fig. 4A, B).

The internal cortex of the shell elements of *Podocnemis erythrocephala* consist of lamellar bone with growth marks that, under polarized light, show a very distinct light and dark layering (Fig. 4E, F). Towards the interior cancellous bone, the light and dark layers increase in thickness (see Fig. 4F), and the layering coincides with the growth marks (Fig. 4E, F). The congruence between layers and growth marks is not that clear in the internal-most part of the internal cortex. Here, bone lamellae that have predominantly small round-shaped bone cell lacunae alternate with bone lamellae, in which the bone cell lacunae are flat and elongated, thus indicating that the lamellar bone tissue has an orthogonal plywood structure. Canaliculi are seldom found. Sharpey's fibers are present throughout the whole of the internal cortex in the thin-section of the sampled hypoplastron. In the costals, Sharpey's fibers are restricted to areas next to the incorporated ribs. Sharpey's fibers were not found in the thin-sections of the sampled peripheral and the neural.

Bone histology of *Bothremys barberi* (Schmidt, 1940), *Taphrosphys sulcatus* (Leidy, 1856), and of "*Foxemys* cf. *F. mechinorum*" Tong, Gaffney, and Buffetaut, 1998 = *Polysternon mechinorum* (Tong, Gaffney, and Buffetaut, 1998) *fide* Lapparent de Broin (2001). —The bone histology of these three taxa is rather similar which is why they are described together. In all samples of *B. barberi*, *T. sulcatus*, and "*Foxemys* cf. *F. mechinorum*", the internal cortices are significantly thinner than the external cortices. A symmetrical diploe build of the bony shells in which the cortices have rather similar thicknesses, is not developed (Fig. 2D–F).

The massive external cortex of all sampled elements is composed of interwoven structural fiber bundles (Fig. 5A$_1$, A$_2$). Cyclical growth marks are best preserved in the neurals. In the neural of *T. sulcatus,* about 20 growth marks were counted (Fig. 5B$_1$). The neural of *B. barberi* has a maximum of nine growth marks and the neural of "*Foxemys*" has six growth marks. Several shell elements of *T. sulcatus* further show a peculiar bone tissue within the external cortices where, locally, the growth marks of the primary bone tissue of the cortices were substituted by secondary bone tissue (Fig. 5B$_2$). Here, the secondary bone appears in an inverted triangular-shaped or hemispherical area with a reticular vascularization pattern. The bone surface directly above the peculiar bone tissue often has a pitted or rugose texture.

The fibrous tissue of the external cortices is dominated by diagonally arranged collagen fiber bundles. Irregularly arranged primary osteons are commonly found throughout the external cortex. Additionally, collagenous fiber bundles that trend perpendicular to the bone surface are incorporated in all layers of the external cortices (Fig. 5A$_1$, A$_2$). Scattered secondary osteons are also present, but they are restricted to the interior-most layer of the external cortex. No secondary osteon clusters were found. Primary canals comprise either single or branching tubules that often point towards the external surface of the bone. Bone cell lacunae are slightly elongated in the external-most layers of the external cortex and more round towards the cancellous bone.

The trabeculae of the interior cancellous bone are composed of secondary lamellar bone with remnants of primary fibrous tissue restricted to interstitial areas of the trabeculae (Fig. 5B$_1$, B$_2$). Bone cell lacunae are common in the interstitial areas and rather sparsely distributed in the secondary lamellar bone of the trabeculae.

The internal cortices are usually composed of a thin zone of parallel-fibered bone (Fig. 5B$_3$, B$_4$). Secondary osteon clusters are not developed in the internal cortices. Sharpey's fibers do occur that are angled towards the surface of the bone (Fig. 5B$_3$, B$_4$) in the internal cortices of both neurals and costals of *T. sulcatus* and *B. barberi*.

Bone histology of *Pelomedusa subrufa* (Bonnaterre, 1789). —The samples of *P. subrufa* have a diploe build with well-developed cortices and interior cancellous bone (Figs. 2G, 6A). Below thin layers of keratin that compose the shield cover and a very thin layer of unossified tissue, the surface of the underlying bone is slightly pitted. Cyclic growth is also present in the keratinous shield. Instead of following the pit-

Fig. 4. Bone histology of *Podocnemis erythrocephala* (Spix, 1824). Sampled costal (YPM 11853) of *Podocnemis erythrocephala* (Spix, 1824), the Recent red-headed Amazon River turtle, South America (provenance unknown). **A**. Photomicrograph of thin-section in polarized light. The diploe structure of the shell is clearly visible. Cortices are of similar size and show growth marks. The interior cancellous bone is largely remodeled by secondary osteons. **B**. Detail of external cortex in polarized light showing a succession of growth marks (small white arrows) in the interwoven fibrous bone tissue disturbed by a semicircular area of secondary bone remodeling. **C**. Close-up of the margin of remodeled area seen in B in normal transmitted light. Note the scalloped line and adjacent bone cell lacunae between the primary tissue with growth marks and the secondary bone. **D**. Same view as in C, seen in polarized light. The →

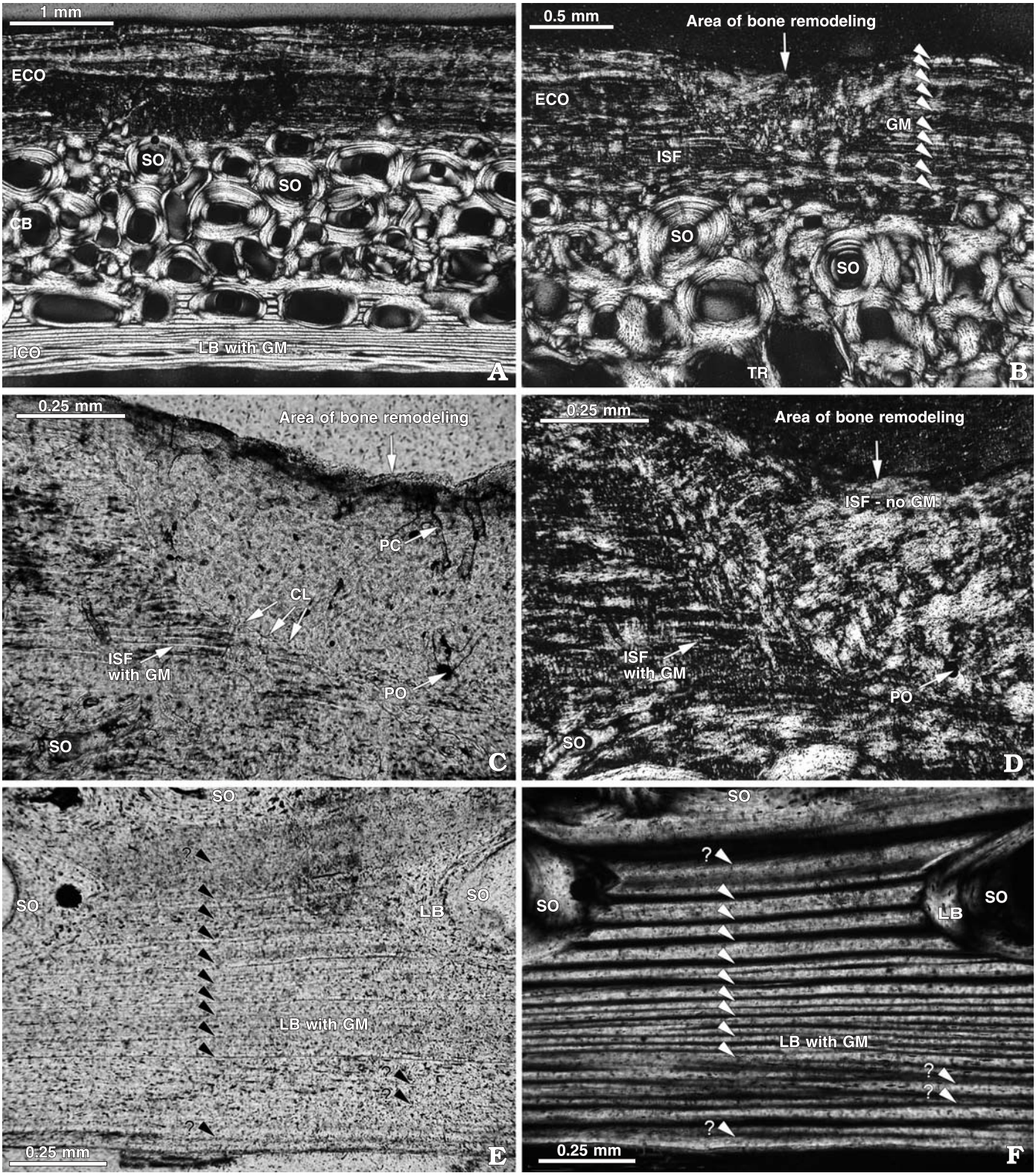

remodeled area of bone also constitutes interwoven structural fibers, but growth marks are not present. **E**. Detail of internal cortex in normal transmitte light. Note the growth marks in the lamellar bone tissue. **F**. Same view as in E, seen in polarized light. Note the clearly distinguished light and dark layering of the cortical bone. Growth marks (small white arrows) have been transferred from E to verify that the light and dark layers in the interior part of the cortex next to the cancellous bone coincide with the growth marks. Light and dark layers in the internal part of the cortex do not always coincide with the growth marks, but constitute lamellae of the lamellar bone tissue. Note that some growth marks appear discontinuous in the cortical bone tissue (marked with question marks). Abbreviations: CB, cancellous bone; CL, bone cell lacunae; ECO, external cortex; GM, growth marks; ICO, internal cortex; ISF, interwoven structural collagenous fiber bundles; LB, lamellar bone tissue; PC, primary vascular canal; PO, primary osteon; SO, secondary osteon; TR, bone trabeculae.

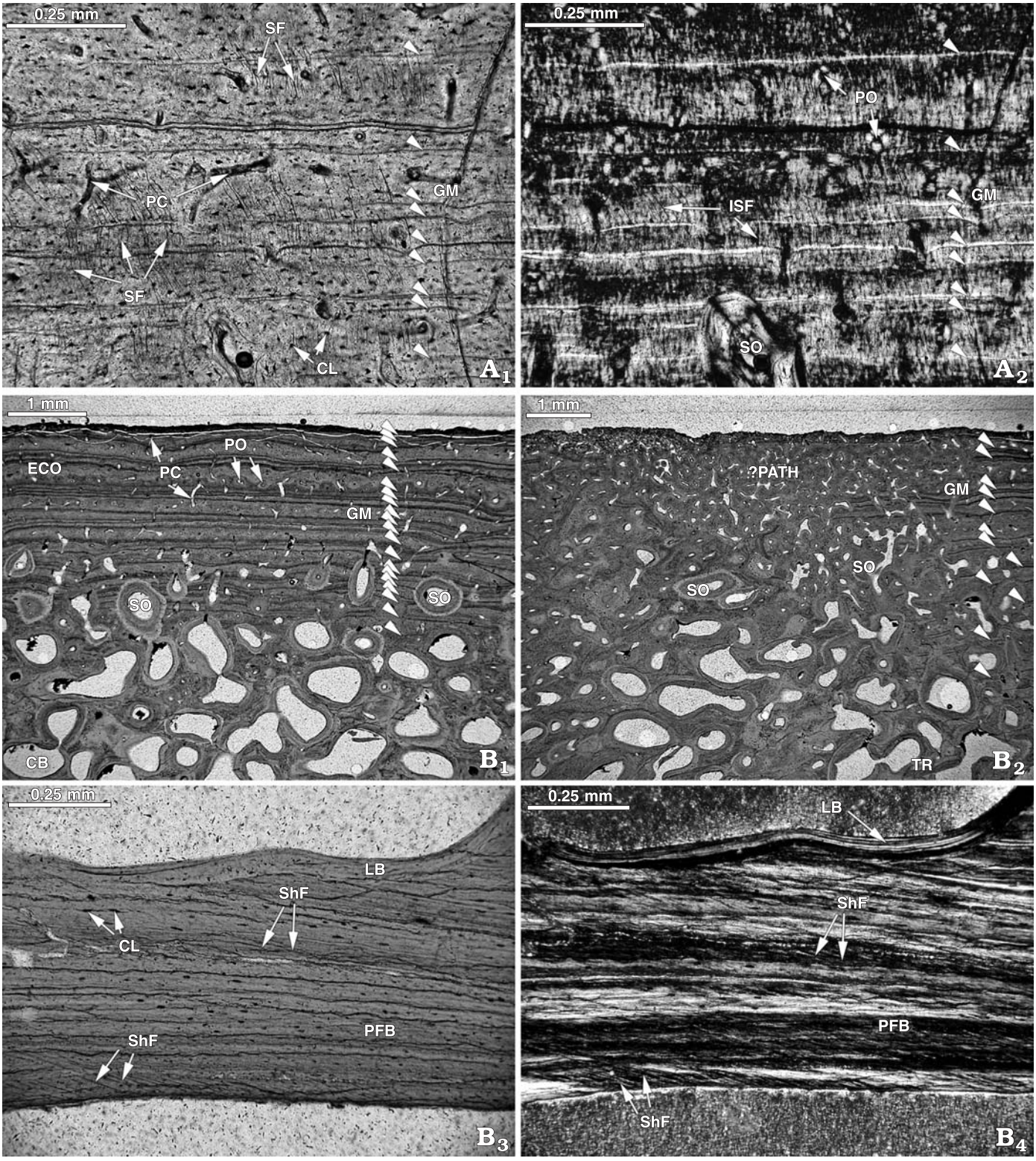

Fig. 5. Bone histology of the bothremydid turtles *Bothremys barberi* (Schmidt, 1940) and *Taphrosphys sulcatus* (Leidy, 1856). **A**. Sampled costal (FM P27406) of *Bothremys barberi* (Schmidt, 1940), Campanian (Late Cretaceous) Mooreville Chalk, Selma Group, Dallas County, Alabama, USA. A_1. External cortex observed in normal light. Widely spaced growth marks are found in this detail of the cortex. The bone tissue in between the growth marks is vascularized by primary osteons or branching primary canals. Structural fiber bundles that trend perpendicular to the surface of the bone are found throughout the whole of the cortex. A_2. Same view as in A_1, seen in polarized light. Perpendicular fiber bundles cross the interwoven structural fiber bundles. Note that not all growth marks (small white arrows) appear as bright, birefringent lines in the fibrous tissue. **B**. Sampled neural (YPM 40288) of *Taphrosphys sulcatus* (Leidy, 1856), Late Cretaceous, New Jersey, USA. B_1. External cortex and external part of cancellous bone are observed in normal light. The cortical bone has 20 growth marks (small white arrows). Vascularization is accomplished through primary osteons and primary canals. →

ted course of the bone, the unossified tissue expands into the pits and fills them (Fig. 6B). The external cortex expresses a few weakly developed growth marks. It is composed of interwoven collagenous fiber bundles regularly interspersed with primary osteons. Scattered secondary osteons are seldom found. Fiber bundles perpendicular to the bone surface can be found throughout the external cortex. They are most clearly visible right below the border where bone meets connective tissue. The orientation of the fiber bundles is predominantly subparallel or diagonal to the external surface of the bone. Bone cell lacunae are mostly round to slightly elongated, and they usually do not bear any canaliculi.

The interior cancellous bone consists of bone trabeculae and patches of interstitial primary bone that are still quite large. The trabeculae are thinly lined with endosteal lamellar bone. Bone cell lacunae are plump and round in shape in the interstitial areas and slightly elongated within the bone lamellae.

The internal surface of the bone is covered with a thin layer of soft connective tissue (Fig. 6C). The internal compact bone itself is avascular and constitutes parallel-fibered bone tissue. Bone cell lacunae in the interior cortical bone are rather flat and elongated and mostly follow the layering of the bone lamellae (Fig. 6C).

Bone histology of *Hesperotestudo* (*Caudochelys*) *crassiscutata* (Leidy, 1889).—The bone histology of *H. crassiscutata* is characterized by the typical diploe build. Internal and external compact bone layers are of similar thickness and delineate an interior area of cancellous bone (Figs. 2H, 7A). All samples had a shallow but rough texture of the external

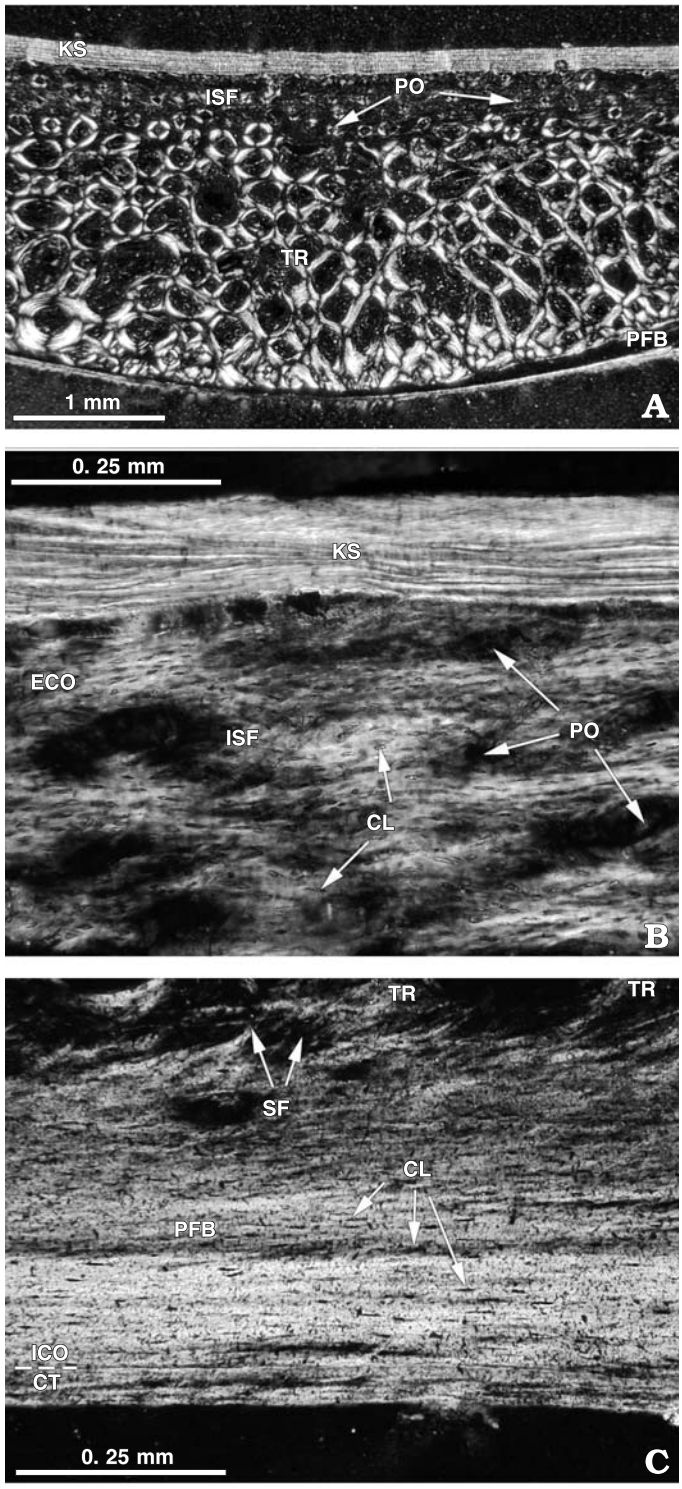

Fig. 6. Bone histology of *Pelomedusa subrufa* (Bonnaterre, 1789); Recent, Africa (provenance unknown). Thin-section of a sampled costal (MVZ 230517). **A**. The whole of the thin-section observed in polarized light. The diploe build of the shell is apparent below a keratinous shield (see also Fig. 2G). Only a thin layer of connective tissue is present in between the shield tissue and the bone tissue. The plane of sectioning lies perpendicular to the incorporated rib in the costal. In the thin-section, the former rib is only seen as a dorsoventrally thickened amount of cancellous bone and the slightly curved internal cortex. **B**. Detail of the external cortex of the costal in polarized light where the interwoven fiber bundles are interspersed with primary osteons. Bone cell lacunae that appear within the whole of the cortical bone are rather of round shapes. **C**. Detail of the parallel-fibered bone of the internal cortex of the costal. Below the surface of the bone, a thin layer of fibrous connective tissue is still present. Abbreviations: CL, bone cell lacunae; CT, connective tissue; ECO, external cortex; ICO, internal cortex; ISF, interwoven structural collagenous fiber bundles; KS, keratinous shield; PFB, parallel-fibered bone; PO, primary osteon, SF, structural collagenous fiber bundles; TR, bone trabeculae.

The amount and size of secondary osteons is increasing towards the interior cancellous bone. B_2. Detail of the same external cortex as in B_1, where growth marks are disturbed by secondary bone remodeling. The remodeled area, hypothesized to represent a pathology, is well vascularized and constitutes interwoven structural fibers. B_3. Internal cortex observed in normal light. Few Sharpey's fibers cross the avascular parallel-fibered cortical bone at moderate angles. B_4. Same detail as in B_3, observed in polarized light. The Sharpey's fibers as well as the endosteal lamellar bone that lines the vascular spaces in the cancellous bone appear much more distinct. Abbreviations: CB, cancellous bone; CL, bone cell lacunae; EC, erosion cavity; ECO, external cortex; GM, growth marks; ISF, interwoven structural collagenous fiber bundles; LB, lamellar bone tissue; ?PATH, putative area of pathology; PC, primary vascular canal; PFB, parallel-fibered bone; PO, primary osteon, SF, structural collagenous fiber bundles; ShF, Sharpey's fibers; SO, secondary osteon; TR, bone trabeculae.

surfaces (Fig. 7A$_1$, A$_2$). The internal surfaces of the bones were generally smooth (Fig. 7A$_3$, A$_4$). Growth marks occur in both cortices, but they are often convoluted or discontinuous. Scattered secondary osteons are an uncommon feature in both the internal and external cortices. They increase in size and number in the compact bone layers situated immediately next to the interior cancellous bone, as those cortical layers are first remodeled and vascularized with growth and increasing age of the turtle.

The external cortex is characterized by an interwoven fibrous bone tissue of bundled collagenous structural fibers. Depending on the exact plane of sectioning, the fiber bundles seem to resemble a well-ordered close-knit fabric (Fig. 7A$_2$). Vascularization occurs through numerous primary osteons and branching primary canals. Many of the primary canals open up towards the surface of the bone, causing the rough texture of the external cortex (Fig. 7A$_1$, A$_2$).

The bone trabeculae of the cancellous bone are rather long and thin and they are lined with periosteal, centripetally deposited lamellar bone towards the vascular spaces (Fig. 7A$_1$, A$_2$), resulting in a well-vascularized meshwork. Some vascular spaces of irregular shape in the trabecular meshwork do not yet have a lining with endosteal lamellar bone. Interwoven collagenous fiber bundles that are usually preserved in the interstitial areas of the bone trabeculae lend the bone trabeculae a close-knit appearance (Fig. 7A$_4$).

The internal cortex is mainly avascular. Only occasionally, a scattered primary osteon or a primary vascular canal is found in the cortical bone. The internal cortex constitutes parallel-fibered bone with local transitions into lamellar bone (Fig. 7A$_4$). In polarized light, many fiber bundles in the bone matrix are angled towards the internal surface of the bone, indicating the presence of Sharpey's fibers (Fig. 7A$_4$). Elongated and irregular shaped bone cell lacunae are clustered and do not follow the trend of the bone lamellae of the internal cortex.

Bone histology of *Archelon ischyros* Wieland, 1896.—A detailed analysis of the bone histology of *A. ischyros* and other marine turtles is beyond the scope of this paper, thus only a preliminary comparison is made (Fig. 2I).

The bone histology of *A. ischyros* is strikingly divergent from that of all other sampled turtle shell elements. A clear histological division between compact bone layers and interior cancellous bone (Fig. 7B$_1$, B$_2$) is not seen. Instead, the boundaries between cortex and cancellous bone are lost in favor of a single, more homogeneous bone tissue of cancellous appearance. The cortices of the bone are not compact but comprise primary cancellous bone tissue with cyclical growth marks. Secondary remodeling processes further enlarge the vascular spaces within the cortices and the cancellous bone. No clustered secondary osteons were found in *A. ischyros*.

Discussion

General growth of shell bone.—The bone histological data presented herein in addition to embryological and developmental data (e.g., Vallén 1942; Kälin 1945; Suzuki 1963; Zangerl 1969; Ewert 1985; see also Hall 2005), allows us to draw some general conclusions about the formation of bones of the turtle shell. While early in ontogeny, the keratinous shields develop fully prior to hatching, the shell bones below the shields still largely have to form (see Zangerl 1969). The earliest bones to ossify in the turtle shell are the elements of the plastron (Rieppel 1993; Sheil 2003).

Only the costals and the neurals develop as a mixture of dermal and endoskeletal bone. All other bony elements of the carapace (e.g., nuchal, pygal, suprapygals, peripherals), the elements of the bridge and the plastron (i.e., epi-, ento-, hyo-, (meso-), hypo-, and xiphiplastra) are of dermal origin (e.g., Zangerl 1969). Because only costals and a neural fragment of *S. geographicus* were sampled, we limit our conclusions to the development of these bone elements. Kälin (1945), Suzuki (1963), and Ewert (1985) give exemplary descriptions of the development of neurals and costals during early ontogenesis. The ossification of the costal starts at the cartilaginous rod of the rib that is sheathed in a thin periosteum, while in the neural the ossification begins at the neural arch (e.g., Vallén 1942; Suzuki 1963; Cherepanov 1997). In both shell elements, lateral-trending consolidation of the mesenchymal parts in the soft tissue of the dermis leads to a preformation of a three-dimensional spongy meshwork in the integument. Concurrently, small bone spiculae grow laterally from the periosteum of the rib into the adjacent dermal layers (e.g., Suzuki 1963), and a periosteum is directly involved in the bone formation only in this initial stage (see Kälin 1945). The successive ossification then proceeds along the mesenchymal aggregations, forming a primary cancellous bone structure and a incipient internal cortical bone layer by intramembraneous ossification (e.g., Suzuki 1963; Zangerl 1969; Cherepanov 1997). The interstitial primary bone tissue, found in the bone trabeculae of all studied thin-sections, provides evidence that the interior cancellous bone is truly a primary structure.

In a second step, the internal cortical bone increases in thickness while the external cortical bone layer begins to develop, thus framing the interior area of cancellous bone. In-

Fig. 7. Bone histology of *Hesperotestudo* (*Caudochelys*) *crassiscutata* (Leidy, 1889) and *Archelon ischyros* Wieland, 1896. **A**. Sampled costal (ROM 55400) of *Hesperotestudo* (*Caudochelys*) *crassiscutata* (Leidy, 1889), Pleistocene of Florida, USA. A$_1$. External cortex observed in normal transmitted light. Vascularization of the cortical bone is observed in form of primary osteons and straight or branching primary canals. Larger scattered secondary osteons are only developed in the direct vicinity of the interior cancellous bone A$_2$. Same detail as in A$_1$, observed in polarized light. Interwoven structural fiber bundles appear like a closely knit fabric. Note how some primary osteons trend almost perpendicular to the surface of the bone. A$_3$. Internal cortex observed in normal light. Note that the layers next to the surface of the bone are sparsely vascularized. Rounded bone cell lacunae appear in clusters in the →

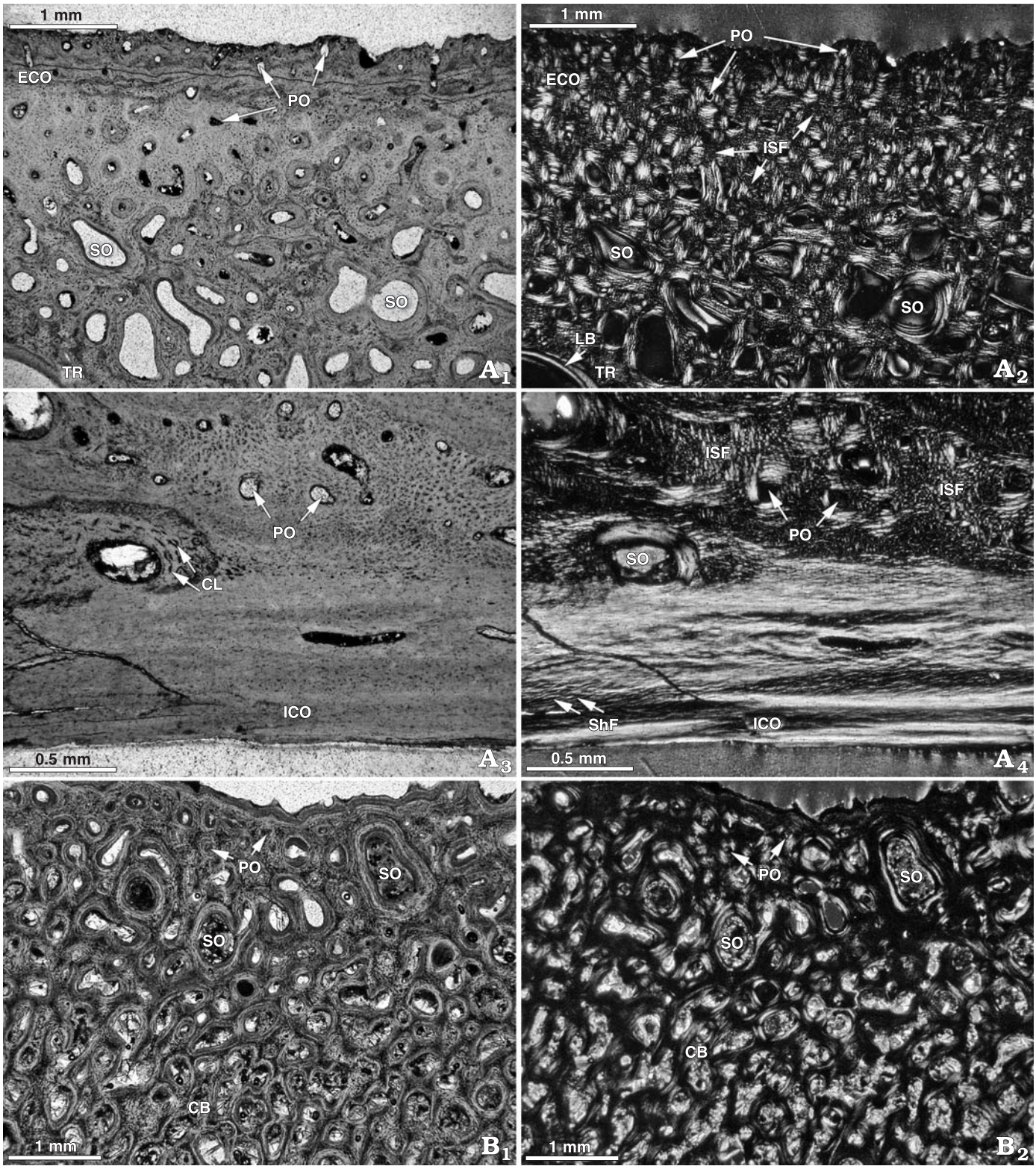

cortical bone, whereas they are flattened in the scattered secondary osteons and follow the centripetally deposited bone lamellae. A_4. Same detail as in A_3 observed in polarized light. Note the fibrous appearance next to the surface of the bone. Large areas of primary interstitial bone of interwoven fiber bundles (again resembling close-knit fabrics) interspersed with primary and secondary osteons occur in the interior regions of the cortex. **B**. Sampled shell fragment (YPM 1783) of *A. ischyros*, Wieland, 1896 from the Late Cretaceous of South Dakota, USA. B_1. Thin-section observed in normal transmitted light. The whole bone tissue is mostly primary and uniformly spongy in appearance. No discrete division into cancellous and cortical bone can be observed. B_2. Same detail as in B_1, observed in polarized light. Abbreviations: CB, cancellous bone; CL, bone cell lacunae; ECO, external cortex; ICO, internal cortex; ISF, interwoven structural collagenous fiber bundles; LB, lamellar bone tissue; PO, primary osteon; ShF, Sharpey's fibers; SO, secondary osteon; TR, bone trabeculae.

ternal and external bone layers of the diploe shell bone reflect distinct dermal structures with different collagenous fiber bundle orientations (see also Zangerl 1969). However, in contrast to Zangerl (1969: 313), our study shows that the cortical bone layers of the shell diploe cannot be described simply as "zones of lamellar bone, containing moderately numerous radial vascular canals". Instead, the internal and external cortices are clearly distinct from each other—the external cortical layer is not comprised of lamellar bone at all. Furthermore, radial vascular canals are not seen in any of our histological samples. In the studied Bothremydidae, the internal cortices gain less in thickness relative to the external bone cortex, their development is delayed.

Although the studied turtle shell fragments of *Stupendemys geographicus* originate from among the thickest and largest turtle shells known (Wood 1976), their histological structure is generally simple. A well-developed diploe structure of the shell bones is discovered in all fragments (Zangerl 1969). Whereas a simple compact domed shell would suffice for a turtle to give its shell enough form stability, especially for larger and ultimately for giant-sized turtles it becomes increasingly important to minimize shell weight during growth due to scaling effects. As seen in *Hesperotestudo crassiscutata* and *S. geographicus*, the diploe structure presents such a way of lightweight construction. Form stability and the moment of inertia (in this case, the capacity of the turtle shell to resist bending stresses) of the domed shell is maintained, because the compact bone layers serve as tension-resistant layers around the meshwork of interior cancellous bone. This seems even more relevant for land-dwelling tortoises than for turtles that experience buoyancy in freshwater and marine habitats for the majority of their lives. This fact can also be inferred from the comparison of *S. geographicus* and *H. crassiscutata*, because the vascularization in the tortoise exceeds that of the pleurodire turtle. A diploe structure of the bony shell was encountered in all sampled taxa except the bothremydid turtles and *Archelon ischyros*. In the case of *Bothremys barberi*, *Taphrosphys sulcatus*, and "*Foxemys* cf. *F. mechinorum*", this structure is lost due to the reduction of the internal cortex revealing a potential synapomorphy for Bothremydidae.

The uniform primary spongy appearance of the whole shell bone tissue of *A. ischyros* is comparable to endoskeletal bone structures recognized in some tetrapod groups (e.g., ichthyosaurs, dolphins) secondarily associated with an open marine lifestyle (Buffrénil et al. 1987; Buffrénil and Schoevaert 1988; Ricqlès 1989; Buffrénil and Mazin 1990; Ricqlès and Buffrénil 2001). The osteoporoitic trend in the shell of *A. ischyros* is hypothesized to lead to a weight-reduced shell skeleton with lower mass and density (compare to Taylor 2000), a characteristic further enhanced by the enormous morphological reduction of the shell elements and the presence of large fontanelles. Long bone microstructure of *A. ischyros* relates to fast growth and large size while that of the long bones of *S. geographicus* indicate also large size but slow growth (Rhodin 1985). Although both turtles thus reach similar giant size classes, the strongly functional aspects tied to an open marine habitat in *A. ischyros* further prevent resolution of size-related constraints in the shell bone histology of *S. geographicus*.

Compact bone.—In general, the external cortex of the turtle shell, but not the internal cortical bone (this study; Scheyer et al. in press) is composed of metaplastic bone tissue, i.e., interwoven structural fiber bundles of the dermis (Haines and Mohuiddin 1968). Metaplastic ossification as a mode of osteogenesis in osteoderms was already discussed e.g., in lepidosaurs (Levrat-Calviac and Zylberberg 1986) and archosaurs (Scheyer and Sander 2004; Main et al. 2005). The fact that in *S. geographicus* not only the external cortex but also the internal-most layers of the internal cortex are partly composed of ossified metaplastic connective tissue is apomorphic in the phylogenetic context. The presence of the metaplastic tissue in the internal cortex in *S. geographicus* may be related to the extreme thickness of the shell elements, although other studied giant turtles with similar shell thicknesses do not show this feature.

The distinct cyclical growth marks in the lamellar bone of the internal cortex of *Podocnemis erythrocephala*, perceived as a black and white layering, is not encountered in the other sampled specimens and is thus treated as a potential apomorphy for this taxon. Whereas the layering resembles true bone lamellae in the internal-most part of the lamellar bone, the interior-most dark and light layers that coincide exactly with the growth marks are too thick to represent the bone lamellae of the lamellar bone tissue. In either case, the lamellar bone matrix found in the samples of *P. erythrocephala* indicates low osteogenetic rates, while most other taxa with a parallel-fibered bone matrix experienced intermediate rates of osteogenesis. While true woven-fibered bone (e.g., in long bones) with its irregular and loosely packed collagen fiber arrangement and general isotropy in polarized light is typically associated with rapid osteogenesis (Francillon-Vieillot et al. 1990), the same cannot be assumed for the metaplastic tissue of interwoven structural fiber bundles recognized in the external cortex of the turtle shell (well ordered fiber bundle arrangement, no general isotropy), for which detailed bone formation rates are not yet available.

Based on the comparison of *S. geographicus* with the Recent taxa *Podocnemis erythrocephala* and *Pelomedusa subrufa*, fiber bundles that insert perpendicular to the external bone surfaces found in the fossil taxa are hypothesized as a means of physically strengthening the interface of the keratinous shield cover and the underlying bony shell, with only a very thin layer of fibrous connective tissue being present in between. The cortices of *Stupendemys geographicus* are strongly vascularized. The cortical bone of all other pelomedusoid turtles is mainly avascular. However, because heavy remodeling of the bone usually leads to the formation and accumulation of successive generations of secondary osteons, called Haversian bone, with progressive age (e.g., Francillon-Vieillot et al. 1990) and thus higher

vascularization, the observed bone histology of *S. geographicus* appears to be directly influenced not only by its large size but also by its old age.

Interior cancellous bone.—Differences in the cancellous bone of the specimens of *S. geographicus* with other pelomedusoid taxa, are mainly restricted to trabecular thickness and width of vascular spaces, characters that are known to vary between differently sized and aged individuals. With progressing age, primary bone features, like remnants of areas of interstitial bone or primary bone lamellae are successively erased through continued remodeling and vascularization processes.

Growth marks.—All of the sampled turtles did exhibit cyclical growth patterns in the bone tissue. Although to our knowledge, seasonal origin of the growth marks in pleurodiran turtle shell bones has not been proven, it seems most likely that they are annual in nature. Neurals with their extensive record of growth marks seem the most useful of the shell elements if age assessment would be attempted in connection with skeletochronology based on long bone histology. In case of the Recent *Podocnemis erythrocephala* and *Pelomedusa subrufa*, the growth patterns are not as conspicuous as in the fossil taxa. This seems to be related to differences in preservation between the modern bone, where the collagen content is still present, and the fossilized bone that is almost completely permineralized. In *Taphrosphys sulcatus*, the observed growth marks become more condensed towards the external surface of the bone, giving the impression of an old and matured bone. In *S. geographicus*, the observed growth marks do not give this impression, because they are evenly spaced throughout the cortical bone. Furthermore, it has to be taken into account that the record of growth marks is not complete due to the weathering that the specimens of *S. geographicus* undoubtedly experienced.

Age and growth estimates.—Numerous scientific approaches have been carried out over the last decades to assess and validate the age and growth of turtles based on skeletochronological evidence (e.g., Castanet et al. 1979; Zug et al. 1986; Castanet 1987, 1988; Klinger and Musick 1992, 1995; Zug and Parham 1996; Zug and Glor 1998; Coles et al. 2001; Zug et al. 2001; Snover and Hohn 2004). Most of these works focused on marine turtles and tortoises, the two turtle taxa that include some of the largest living turtles today. Zug and Parham (1996) predicted growth rates for the largest living turtle, the marine leatherback *Dermochelys coriacea*, from 349 mm/yr for individuals during their first year to 86 mm/yr for individuals from four to seven years in age. With "average juvenile growth rates exceeding 8.5 cm/yr […], *Dermochelys* has the fastest growth of living turtles" (Zug and Parham 1996: 246).

According to Rhodin (1985), who studied chondro-osseous growth in endoskeletal bones of fossil and Recent turtles, *Archelon ischyros* showed significant histological similarities (e.g., vascularized cartilage) with the rapidly growing *D. coriacea*. *S. geographicus* on the other hand lacked comparable features, instead showing a microstructure similar to Recent turtles with a "normal", slow mode of growth (Rhodin 1985).

Applying the growth rates of *D. coriacea* to the presumably "slow-growing" *S. geographicus*, it would have taken the giant pleurodire turtle a minimum of 30 years to reach a SCL of 3.3 meters. If slower, possibly more realistic, mean growth rates of 30–53 mm/yr "for most age and size classes" of the cheloniid turtle *Chelonia mydas* are applied (Zug and Glor 1998: 1497), the age estimates would increase to 60 to 110 years. Similar estimates would be obtained when calculating with growth values of the cheloniid *Caretta caretta* (e.g., Klinger and Musick 1995: ~53 mm/yr to ~29 mm/yr for 400–1000 mm SCL). The difference between the histologically visible growth record and real age becomes even more pronounced, considering that all turtles further decrease growth towards maturity and old age (e.g., Peters 1983; Klinger and Musick 1995; Zug et al. 2001).

Sharpey's fibers.—Sharpey's fibers that cross the metaplastically ossified connective tissue in the external cortices and the bone lamellae of the internal cortices are present within the carapace fragments of all sampled turtle taxa except in *A. ischyros*. The Sharpey's fibers in the external cortices seem to be uniformly connected with the anchoring of an overlying layer of connective tissue and the keratinous shields to the underlying bony shell. Sharpey's fibers that cross the internal cortices at low to medium angles within the costals and the lateral parts of the neurals are hypothesized to be associated with the carapacial attachment of the musculus transversus abdominis, one of the major muscles associated with turtle lung ventilation (see Landberg 2003: fig. 1).

Unusual bone growth.—The only secondary osteon clusters that seem to be part of the normal bone forming process of the shell were found in *S. geographicus*. The secondary bone remodeling in *Podocnemis erythrocephala* and in the fossil *Taphrosphys sulcatus*, on the other hand, deviate from general external cortical bone tissue of turtle shells. As observed in modern turtle taxa (e.g., *P. erythrocephala*), a possible reason for such unusual secondary bone deposition could be a reaction to incipient osteomyelitis or "shell rot" (e.g., Frye 1991; Sinn 2004). Often following trauma, microbes enter spaces between the keratinous shields and the underlying bone becomes infected. Similar pathologies, i.e., pitting and other lesions of the turtle shell bone, have already been described in fossil turtles from the Eocene of Wyoming, North America (Hutchison and Frye 2001). As inferred from modern turtles that are highly aquatic, phenomena like "shell rot" in fossil turtles can also be related to poor water quality (see also discussion in Hutchison and Frye 2001).

Systematic value.—In general, bone histology yields data that are of potential use in studies of turtle phylogeny (Scheyer et al. in press). Among pelomedusoid pleurodires, the diploe build of the shell (see Fig. 2H) and bone tissue that consists of

interwoven structural collagenous fiber bundles are hypothesized to be plesiomorphic characters. The same applies to the development of growth marks in the turtle shell elements. Growth marks were encountered in all sampled taxa, including the cryptodiran turtles *Hesperotestudo crassiscutata* and *Archelon ischyros*. A reduction in the thickness of the internal cortex in pelomedusoides turtles is only found among Bothremydidae, thus constituting a potential synapomorphy of this group. Secondary osteon clusters in the internal cortex of *Stupendemys geographicus* or the distinguished dark and light layering of the internal cortex of *Podocnemis erythrocephala* in polarized light are apomorphic characters for those taxa, respectively. Variation in the shell structures of the pelomedusoides turtles that may be size-related (biomechanical stress-related) instead of related to taxonomy cannot be ruled out. However, based on the lack of data available on stress-induced variation of the bone microstructures of different aquatic and terrestrial turtle taxa of varying ontogenetic stages and size classes, it cannot be verified at this time.

Conclusion

The comparison of histological samples led to the conclusion that the truly giant size of *Stupendemys geographicus* was not based upon a novel way of shell bone formation that greatly differs to that of other turtles in general. The diploe structure of the shell together with well-developed external and internal cortices is plesiomorphic for the turtles studied. The assignment of *S. geographicus* to the Podocnemidae was neither refuted nor supported by the bone histological results. Cyclic growth is apparent in all sampled taxa, however, in the case of *S. geographicus* the bias between countable to resorbed growth marks, and the lack of a long bone growth record make age estimates extremely difficult. Comparison with growth rates of modern marine turtles leads to the hypothesis that *S. geographicus* is likely to have grown for at least three decades in order to reach truly giant sizes with carapace lengths well over three meters.

Acknowledgments

Our gratitude goes to Walter Joyce and Jacques Gauthier (both at Yale Peabody Museum, New Haven, USA), Olivier Rieppel and associates (Field Museum, Chicago, USA), Kevin Seymour (Royal Ontario Museum, Toronto, Canada), Hayan Tong and Eric Buffetaut (both at the Centre National de la Recherche Scientifique, Paris, France), Orangel Aguilera (Centre of Archaeology, Anthropology and Paleontology of Francisco de Miranda University, Coro, Venezuela), and to Chris Conroy and associates (Museum of Vertebrate Zoology, University of California, Berkeley, USA), for the possibility to obtain specimens for histological sampling. Furthermore, TMS would like thank Martin Sander (University of Bonn, Germany), for his supervision and support, and Nicole Klein and Elke Goldbeck (University of Bonn, Germany), for discussions and for reading earlier versions of the manuscript. TMS is further indebted to Olaf Dülfer, Ragna Redelstorff, and Dominik Wolff (University of Bonn, Germany) who helped in preparing thin-sections. Finally we would like to thank Walter Joyce and an anonymous reviewer for improving the manuscript. Fieldwork was supported by the Committee for Research and Exploration of the National Geographic Society (Grant 7600-04 to MRSV). The project was funded by the DFG (Grant # SA-469/15-1/2 to TMS and P. Martin Sander).

References

Aguilera Socorro, O.A. 2004. *Tesoros paleontológicos de Venezuela: Urumaco, Patrimonio Natural de la Humanidad*. 148 pp. Arte, Caracas.

Aguilera, O., Sánchez, R., and Terrible, F. 1994. Un nuevo registro de *Stupendemys geographicus* Wood, 1976 (Testudinidae: Pelomedusidae) de la Formación Urumaco (Mioceno Tardío) en el Estado Falcón, Venezuela. Convención Anual de ASOVAC, 54, Coro, UNEFM, *Acta Científica Venezolana, Resúmenes* 45: 333.

Antunes, M.T. and Broin, F. de 1988. Le Crétacé terminal de Beira Litoral, Portugal: remarques stratigraphiques et écologiques, étude complémentaire de *Rosasia soutoi* (Chelonii, Bothremydidae). *Ciências da Terra* 9: 153–200.

Barrett, P.M., Clarke, J.B., Brinkman, D.B., Chapman, S.D., and Ensom, P.C. 2002. Morphology, histology and identification of the "granicones" from the Purbeck Limestone Formation (Lower Cretaceous: Berriasian) of Dorset, southern England. *Cretaceous Research* 23: 279–295.

Bloom, W. and Fawcett, D.W. 1994. *A Textbook of Histology.* 12th Edition. 460 pp. Chapman and Hall, New York.

Bonnaterre, P.J. 1789. *Tableau encyclopédique et méthodique des trois règnes de la nature. Erpétologie.* 72 pp. Panckoucke, Paris.

Broin, F. de 1977. Contribution à l'étude des chéloniens. Chéloniens continentaux du Crétacé et du Tertiaire de France. *Mémoires du Muséum Nationale d'Histoire Naturelle* C38: 1–366.

Broin, F. de 1988. Les tortues et le Gondwana. Examen des rapports entre le fractionnement du Gondwana au Crétacé et la dispersion géographique des tortues pleurodires à partir du Crétacé. *Studia Geologica Salmanticensia, Studia Palaeocheloniologica* 2: 103–142.

Buffrénil, V. de and Mazin, J.-M. 1990. Bone histology of the ichthyosaurs: comparative data and functional interpretation. *Paleobiology* 16: 435–447.

Buffrénil, V. de and Schoevaert, D. 1988. On how the periosteal bone of the delphinid humerus becomes cancellous: ontogeny of a histological specialization. *Journal of Morphology* 198: 149–164.

Buffrénil, V. de, Mazin, J.-M., and Ricqlès, A. de 1987. Caractères structuraux et mode de croissance du fémur d'*Omphalosaurus nisseri*, ichthyosaurien du Trias moyen de Spitzberg. *Annales de Paléontologie (Vert.-Invert.)* 73: 195–216.

Castanet, J. 1987. La squelettochronologie chez les reptiles III – application [with English summary]. *Annales des Sciences Naturelles, Zoologie, Paris* 8: 157–172.

Castanet, J. 1988. Les méthodes d'estimation de l'age chez les chéloniens [with English summary]. *Mésogée* 48: 21–28.

Castanet, J. and Cheylan, M. 1979. Les marques de croissance de l'age chez *Testudo hermanni* et *Testudo graeca* (Reptilia, Chelonia, Testudinidae). *Canadian Journal of Zoology* 57: 1649–1665.

Castanet, J., Francillon-Vieillot, H., Meunier, F.J., and Ricqlès, A. de 1993. Bone and individual aging. *In*: B.K. Hall (ed.), *Bone Volume 7: Bone Growth – B*, 245–283. CRC, Boca Raton.

Cherepanov, G.O. 1997. The origin of the bony shell of turtles as a unique evolutionary model in reptiles. *Russian Journal of Herpetology* 4: 155–162.

Coles, W.C., Musick, J.A., and Williamson, L.A. 2001. Skeletochronology validation from an adult loggerhead (*Caretta caretta*). *Copeia* 1: 240–242.

Ernst, C.H. and Barbour, R.W. 1989. *Turtles of the World*. 313 pp. Smithonian, Washington D.C.

Ewert, M.A. 1985. Embryology of turtles. *In*: C. Gans, F. Billet, and P.F.A. Maderson (eds.), *Biology of the Reptilia. Volume 14—Development A*, 75–268. John Wiley & Sons, New York.

Francillon-Vieillot, H., Buffrénil, V. de, Castanet, J., Géraudie, J., Meunier, F.J., Sire, J.Y., Zylberberg, L., and Ricqlès, A. de 1990. Microstructure and mineralization of vertebrate skeletal tissues. *In*: J.G. Carter (ed.), *Skeletal Biomineralization: Patterns, Processes and Evolutionary Trends*, 471–530. Van Nostrand Reinhold, New York.

Frye, F.L. 1991. *Reptile Care, an Atlas of Diseases and Treatments*. 637 pp. T.F.H. Publications, Neptune City.

Fuente, M. de la 2003. Two new pleurodiran turtles from the Portezuelo Formation (Upper Cretaceous) of Northern Patagonia, Argentina. *Journal of Paleontology* 77: 559–575.

Gaffney, E.S. 1975. A revision of the side-necked turtle *Taphrosphys sulcatus* (Leidy) from the Cretaceous of New Jersey. *American Museum Novitates* 2571: 1–24.

Gaffney, E.S. 2001. *Cearachelys*, a new side-necked turtle (Pelomedusoides: Bothremydidae) from the Early Cretaceous of Brazil. *American Museum Novitates* 3319: 1–20.

Gaffney, E.S. and Forster, C.A. 2003. Side-necked turtle lower jaws (Podocnemididae, Bothremydidae) from the Late Cretaceous Maevarano Formation of Madagascar. *American Museum Novitates* 3397: 1–13.

Gaffney, E.S. and Meylan, P.A. 1988. A phylogeny of turtles. *In*: M.J. Benton (ed.), *The Phylogeny and Classification of the Tetrapods. Volume 1: Amphibians, Reptiles, Birds*, 157–219. Clarendon, Oxford.

Gaffney, E.S. and Zangerl, R. 1968. A revision of chelonian genus *Bothremys* (Pleurodira: Pelomedusidae). *Fieldiana Geology* 16: 193–239.

Gaffney, E.S., Campbell, K.E., and Wood, R.C. 1998. Pelomedusoid side-necked turtles from Late Miocene sediments in Southwestern Amazonia. *American Museum Novitates* 3245: 1–11.

Hailey, A. and Lambert, M.R.K. 2002. Comparative growth patterns in Afrotropical giant tortoises (Reptilia Testudinidae). *Tropical Zoology* 15: 121–139.

Haines, R.W. and Mohuiddin, A. 1968. Metaplastic bone. *Journal of Anatomy* 103: 527–538.

Hall, B.K. 2005. *Bones and Cartilage: Developmental and Evolutionary Skeletal Biology*. 760 pp. Elsevier Academic Press, Amsterdam.

Head, J.J., Raza, S.M., and Gingerich, P.D. 1999. *Drazinderetes tethyensis*, a new large trionychid (Reptilia: Testudines) from the marine Eocene Drazinda Formation of the Sulaiman Range, Punjab (Pakistan). *Contributions from the Museum of Paleontology, the University of Michigan* 30: 199–214.

Hill, R.V. 2005. Integration of morphological data sets for phylogenetic analysis of Amniota: the importance of integumentary characters and increased taxonomic sampling. *Systematic Biology* 54: 530–547.

Hutchison, J.H. and Frye, F.L. 2001. Evidence of pathology in early Cenozoic turtles. *PaleoBios* 21: 12–19.

Joyce, W.G., Parham, J.F., and Gauthier, J.A. 2004. Developing a protocol for the conversion of rank-based taxon names to phylogenetically defined clade names, as exemplified by turtles. *Journal of Paleontology* 78: 989–1013.

Kälin, J. 1945. Zur Morphogenese des Panzers bei den Schildkröten. *Acta Anatomica* 1: 144–176.

Klingenberg, C.P. 1998. Heterochrony and allometry: the analysis of evolutionary change in ontogeny. *Biological Reviews* 73: 79–123.

Klinger, R.C. and Musick, J.A. 1992. Annular growth layers in juvenile loggerhead turtles (*Caretta caretta*). *Bulletin of Marine Science* 51: 224–230.

Klinger, R.C. and Musick, J.A. 1995. Age and growth of loggerhead turtles (*Caretta caretta*) from Chesapeake Bay. *Copeia* 1: 204–209.

Landberg, T., Mailhot, J.D., and Brainerd, E.L. 2003. Lung ventilation during treadmill locomotion in a terrestrial turtle, *Terrapene carolina*. *Journal of Experimental Biology* 206: 3391–3404.

Lapparent de Broin, F. de, Bocquentin, J., and Negri, F.R. 1993. Gigantic turtles (Pleurodira, Podocnemididae) from the Late Miocene–Early Pliocene of South Western Amazon. *Bulletin de l'Institut Français d'Études Andines* 22: 657–670.

Lapparent de Broin, F. de 2001. The European turtle fauna from the Triassic to the Present. *Dumerilia* 4: 155–217.

Leidy, J. 1856. Notices of remains of extinct turtles of New Jersey, collected by Prof. Cook, of the State Geological Survey, under the direction of Dr. W. Kitchell. *Proceedings of the Academy of Natural Sciences of Philadelphia* 8: 303–304.

Leidy, J. 1889. Description of vertebrate remains from Peace Creek, Florida. *Transactions of the Wagner Free Institut of Science of Philadelphia* 7: 13–31.

Levrat-Calviac, V. and Zylberberg, L. 1986. The structure of the osteoderms in the gekko: *Tarentola mauritanica*. *American Journal of Anatomy* 176: 437–446.

Liem, K.F., Bemis, W.E., Walker, W.F. Jr., and Grande, L. 2001. *Functional Anatomy of the Vertebrates—An Evolutionary Perspective*. 703 pp. Harcourt College Publishers, Fort Worth.

Main, R.P., Ricqlès, A. de, Horner, J.R., and Padian, K. 2005. The evolution and function of thyreophoran dinosaur scutes: implications for plate function in stegosaurs. *Paleobiology* 31: 291–314.

Meylan, P.A. 1995. Pleistocene amphibians and reptiles from the Leisey Shell Pit, Hillsborough County, Florida. *Bulletin of the Florida Museum of Natural History* 37 (1): 273–297.

Meylan, P.A. 1996. Skeletal morphology and relationships of the Early Cretaceous side-necked turtle, *Araripemys barretoi* (Testudines: Pelomedusoides: Araripemydidae), from the Santana Formation of Brazil. *Journal of Vertebrate Paleontology* 16: 20–33.

Noonan, B.P. 2000. Does the phylogeny of pelomedusid turtles reflect vicariance due to continental drift? *Journal of Biogeography* 27: 1245–1249.

Peters, R.H. 1983. *The Ecological Implications of Body Size*. 329 pp. Cambridge University Press, Cambridge.

Ricqlès, A. de 1989. Les mécanismes hétérochroniques dans le retour des tétrapodes au milieu aquatique [with English abstract]. *Geobios Mémoire Spécial* 12: 337–348.

Ricqlès, A. de and Buffrénil, V. de 2001. Bone histology, heterochronies and the return of tetrapods to life in water: where are we? *In*: J.-M. Mazin and V. de Buffrénil (eds.), *Secondary Adaptations of Tetrapods to Life in Water*, 289–310. Dr. Fr. Pfeil, München.

Ricqlès, A. de, Pereda Suberbiola, X., Gasparini, Z., and Olivero, E. 2001. Histology of dermal ossifications in an ankylosaurian dinosaur from the Late Cretaceous of Antarctica. *Asociación Paleontológica Argentina. Publicación Especial* 7: 171–174.

Rieppel, O. 1993. Studies on skeleton formation in reptiles: patterns of ossification in the skeleton of *Chelydra serpentina* (Reptilia, Testudines). *Journal of Zoology, London* 231: 487–509.

Sander, P.M. 2000. Longbone histology of the Tendaguru sauropods: implications for growth and biology. *Paleobiology* 26: 466–488.

Scheyer, T.M. and Sander, P.M. 2004. Histology of ankylosaur osteoderms: implications for systematics and function. *Journal of Vertebrate Paleontology* 24: 874–893.

Scheyer, T.M., Sander, P.M., Joyce, W.G., Böhme, W., and Witzel, U. (in press). A plywood structure in the shell of fossil and living soft-shelled turtles (Trionychidae) and its evolutionary implications. *Organisms, Diversity & Evolution*.

Schmidt, K.P. 1940. New turtle of the genus *Podocnemis* from the Cretaceous of Kansas. *Geological series of Field Museum of Natural History* 8: 1–12.

Sheil, C.A. 2003. Osteology and skeletal development of *Apalone spinifera* (Reptilia: Testudines: Trionychidae). *Journal of Morphology* 256: 42–78.

Shimada, K. and Hooks III, G.E. 2004. Shark-bitten protostegid turtles from the Upper Cretaceous Moorville Chalk, Alabama. *Journal of Paleontology* 78: 205–210.

Sinn, A.D. 2004. *Pathologie der Reptilien – eine retrospektive Studie*. 160 pp. Ph.D. thesis, Ludwig-Maximilian-Universität, München [available online at: http://edoc.ub.uni-muenchen.de/archive/00001849/].

Snover, M.L. and Hohn, A.A. 2004. Validation and interpretation of annual skeletal marks in loggerhead (*Caretta caretta*) and Kemp's ridley (*Lepidochelys kempii*) sea turtles. *Fishery Bulletin* 102: 682–692.

Spix, J.B. 1824. *Animalia nova sive species novae Testudinum et Ranarum,*

quas in itinere per Brasiliam annis MDCCCXVII–MDCCCXX jussu et auspiciis Maximiliani Josephi I. Bavariae Regis suscepto collegit et descripsit. 53 pp. F.S. Hübschmann, Monachium.

Suzuki, H.K. 1963. Studies on the osseous system of the slider turtle. *Annals of the New York Academy of Sciences* 109: 351–410.

Taylor, M.A. 2000. Functional significance of bone ballastin in the evolution of buoyancy control strategies by aquatic tetrapods. *Historical Biology* 14: 15–31.

Tong, H. and Gaffney, E.S. 2000. Description of the skull of *Polysternon provinciale* (Matheron, 1869), a side-necked turtle (Pelomedusoides : Bothremydidae) from the Late Cretaceous of Villeveyrac, France. *Oryctos* 3: 9–18.

Tong, H., Gaffney, E.S., and Buffetaut, E. 1998. *Foxemys*, a new side-necked turtle (Bothremydidae: Pelomedusoides) from the Late Cretaceous of France. *American Museum Novitates* 3251: 1–19.

Vallén, E. 1942. Beiträge zur Kenntnis der Ontogenie und der vergleichenden Anatomie des Schildkrötenpanzers. *Acta Zoologica* 23: 1–127.

Wieland, G.R. 1896. *Archelon ischyros*: a new gigantic cryptodire testudinate from the Fort Pierre Cretaceous of South Dakota. *American Journal of Science, Series 4* 2: 399–412.

Wood, R.C. 1976. *Stupendemys geographicus*, the world's largest turtle. *Breviora* 436: 1–31.

Zangerl, R. 1969. The turtle shell. *In*: C. Gans, A. d'A. Bellairs, and T.S. Parsons (eds.), *Biology of the Reptilia. Vol. 1 Morphology A*, 311–339. Academic Press, London.

Zug, G.R. and Glor, R.E. 1998. Estimates of age and growth in a population of green sea turtles (*Chelonia mydas*) from the Indian River lagoon system, Florida: a skeletochronological analysis. *Canadian Journal of Zoology* 76: 1497–1506.

Zug, G.R. and Parham, J.F. 1996. Age and growth in leatherback turtles, *Dermochelys coriacea* (Testudines: Dermochelyidae): a skeletochronological analysis. *Chelonian Conservation and Biology* 2: 244–249.

Zug, G.R., Wynn, A.H., and Ruckdeschel, C. 1986. Age determination of loggerhead sea turtles, *Caretta caretta*, by incremental growth marks in the skeleton. *Smithonian Contributions to Zoology* 427: 1–34.

Zug, G.R., Balazs, G.H., Wetherall, J.A., Parker, D.M., and Murakawa, S.K.K. 2001. Age and growth of Hawaiian green seaturtles (*Chelonia mydas*): an analysis based on skeletochronology. *Fishery Bulletin* 100: 117–127.